Graphene-Based Engine Oil Nanofluids for Tribological Applications

ARTICLE *in* ACS APPLIED MATERIALS & INTERFACES · NOVEMBER 2011

Impact Factor: 6.72 · DOI: 10.1021/am200851z · Source: PubMed

3 AUTHORS:

Eswaraiah Varrla
Nanyang Technological University
16 PUBLICATIONS **480** CITATIONS
SEE PROFILE

Sankaranarayanan Venkataraman
Indian Institute of Technology Madras
118 PUBLICATIONS **809** CITATIONS
SEE PROFILE

Ramaprabhu Sundara
Indian Institute of Technology Madras
57 PUBLICATIONS **1,118** CITATIONS
SEE PROFILE

ACS APPLIED MATERIALS & INTERFACES

RESEARCH ARTICLE

www.acsami.org

Graphene-Based Engine Oil Nanofluids for Tribological Applications

Varrla Eswaraiah,[†,‡] Venkataraman Sankaranarayanan,[‡] and Sundara Ramaprabhu*[,†]

[†]Alternative Energy and Nanotechnology Laboratory, Nanofunctional Materials Technology Center (NFMTC), and [‡]Low Temperature Physics Laboratory, Department of Physics, Indian Institute of Technology Madras, Chennai-600036, India

ABSTRACT: Ultrathin graphene (UG) has been prepared by exfoliation of graphite oxide by a novel technique based on focused solar radiation. Graphene based engine oil nanofluids have been prepared and their frictional characteristics (FC), antiwear (AW), and extreme pressure (EP) properties have been evaluated. The improvement in FC, AW, and EP properties of nanofluids is respectively by 80, 33, and 40% compared with base oil. The enhancement can be attributed to the nanobearing mechanism of graphene in engine oil and ultimate mechanical strength of graphene.

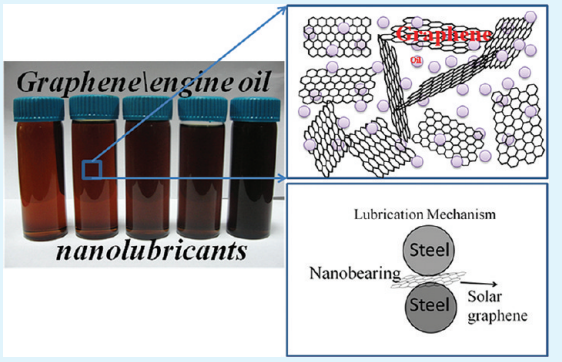

KEYWORDS: graphene, solar exfoliation, frictional coefficient, antiwear, tribology

Graphene, two-dimensional sp^2 carbon atoms arranged in a honeycomb lattice, attracted worldwide interest after its discovery.[1,2] Intrinsically, graphene is a layered structure, quite stiff and exceptionally strong. The fundamental physical properties of graphene especially mechanical strength,[3] tensile stress, thermal conductivity and aspect ratio are enormously high. These excellent properties of graphene make it an advantageous candidate for various applications such as conducting graphene polymer composites for EMI shielding,[4] strain sensor,[5] energy-related applications,[6] and in the bio field.[7] Many methods, including one-step and two-step approaches, have been developed for preparing graphene. The one-step process associates the direct conversion of graphite into graphene occurs,[8] whereas in the two-step process, initially graphite is converted into graphite oxide, and it is further converted into graphene by thermal or chemical reducing agents.[9−11] Recently, we have reported a versatile method for production of highly conducting and ultra-thin graphene by exfoliation of graphite oxide using focused solar radiation (Solar exfoliation technique).[12] Oxygen containing functional groups present in the graphite oxide is inherently present in the graphene[9,10] prepared by the thermal exfoliation of graphite oxide, thus making the graphene partially hydrophilic in nature. On the other hand, the present approach for preparing graphene via solar exfoliation of graphite oxide removes 97% of oxygen from the basal planes of graphite oxide, which makes the sample hydrophobic and help in preparing oil-based nanofluids without any surface treatment.

Friction and wear are the two major causes for energy and material losses in mechanical processes. Lubrication is a principal focus to improve energy efficiency and mechanical durability. Irrespective of the finishing of any metal surface, it contains ridges, valleys, asperities and depressions.[13,14] To improve the effective functioning of mechanical components or two surfaces in contact, better lubricant along with chemical additives is required. In military combat operations, extreme tribological environment is required.[15] For the protection of mechanical components, from friction and wear in aerospace, automotive, military, and various industrial applications, an efficient lubricant is demanded. Moreover, the technology of protecting machines entirely depends on the quality of lubricants. The addition of nanomaterials as additives in base lubricant oil is a rapidly progressing field of research, because nanomaterials are different from traditional bulk materials due to their extremely small size and high specific surface area.[16] Different researchers have tried a variety of nanomaterials (carbon nanotubes, fullerenes and graphite nanosheets) dispersed base oils to improve the antiwear and friction reduction.[17,18] Philip et al.[19] have studied effect of graphite and carbon nanofibers as additives on the performance efficiency of gear pump driven hydraulic circuit using ethanol solution. They claim that both graphite and carbon nanofibers dispersions in ethanol within a concentration range of 195−1500 ppm can maintain hydraulic circuits with increase pump efficiency without modifying the viscosity of the ethanol. Zhang et al.[20] has reported 17 and 14% reduction in frictional coefficient and wear, respectively, with oleic acid-modified graphene as lubricant additive. Ou et al.[21] studied tribological properties of reduced graphene oxide (RGO) sheets on silicon substrate synthesized via covalent assembly. Based on chemical absorption, they have attached reduced graphene oxide to the silicon substrate and microtriboligical behavior of the sample has been evaluated by AFM technique. They attributed the friction reduction and antiwear ability of RGO to its self-lubricating property. Similarly, Lee et al.[22] have demonstrated the generality of the tribological results on thinnest graphene sheets, which indicates that this may be a universal characteristic of nanoscale

Received: June 30, 2011
Accepted: October 8, 2011
Published: October 08, 2011

Scheme 1. Four-Ball Tester and Schematic of Ball-Pot Assembly in Four-Ball Tribotester

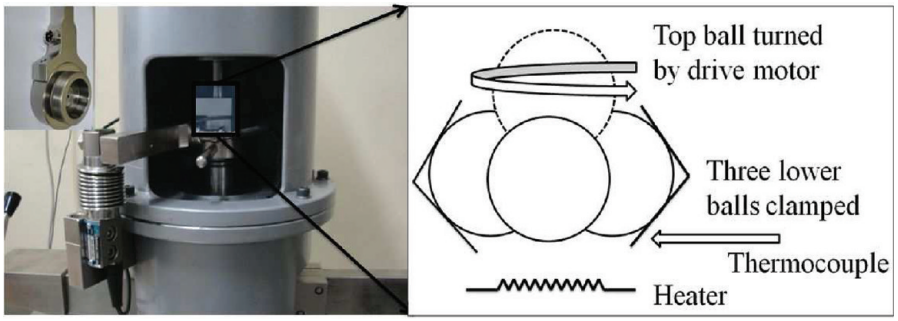

friction for atomically thin materials weakly bound to substrates using frictional force microscopy. Filleter et al[23,24] studied friction and dissipation in epitaxial graphene films on SiC using AFM technique and suggested that graphene films could be used to further reduce friction on SiC surfaces and there are many studies on frictional force microscopy (FFM) of molecules (polymer, single molecules) on different substrates.[25−28] Lin et al.[29] studied the tribological behavior of the lubricating oil containing modified graphene platelets (MGP) was investigated by four ball machine. Pu et al.[30] reported tribological properties of functionalized graphene-ionic liquid nanocomposite films on silicon substrates. In this report, the nanofrictions of the lubrication films were measured using a homemade colloidal probe mounted on the same AFM in contact mode. All these reports show microtribological properties of graphene films over different substrates. From an application point of view, liquid-based nanolubricants are technologically important because of their usage in various industries. Even though reports were already present on liquid-based nanolubricants, they suffer from low efficiency. Hence, it is always essential to improve the efficiency of lubricants. Therefore, we have chosen ultrathin graphene as additive without surfactant or dispersant in engine oils to improve the frictional characteristics and antiwear properties of engine oil.

In the present case, we have prepared highly deoxygenated, less defective ,and super hydrophobic graphene by exfoliation of graphite oxide using focused solar electromagnetic radiation. Without modifying the surface of the graphene, we could successfully disperse this graphene in engine oil with different volume fractions by probe sonicating the nanofluids. Further, after 7 days, we have studied the coefficient of friction, antiwear, and extreme pressure properties of these nanofluids.

EXPERIMENTAL SECTION

Synthesis of Graphite Oxide and Graphene. Graphite Oxide (GO) was prepared according to Modified Hummers method.[31] Graphite (SP-1, Bay Carbon) was used as the starting material. Briefly, graphite was ground with NaCl and washed with DI water followed by filtration. After drying, the filtrate was stirred with conc. H_2SO_4 for 8 h. $KMnO_4$ (6 g) was gradually added while the temperature was kept at less than 20 °C. The mixture was stirred at 40 °C for 30 min. Ninety-two milliliters of water was added to the above solution and heated to ∼100 °C. This was diluted by adding 280 mL of water followed by the addition of 30% H_2O_2. The mixture was washed followed by repeated centrifugation and filtration (first by 5% HCl and then with water). The final product was washed and dried in a vacuum. GO was spread over Petri dish and kept under sunlight. A convex lens of diameter 90 mm was used to focus the incoming radiation from the sun. The power of the focused radiation was ranging from 1.77 to 2.03 W and temperature raised to more than 150 °C within 2−3 s. Material was collected after solar exfoliation and used directly without any modification to the surface.

Characterization Techniques. The Powder XRD measurements were performed with PANalytical X'Pert Pro X-ray diffractometer with nickel-filtered Cu Kα (1.54 Å) radiation as the X-ray source. The pattern was recorded in the 2θ range of 5− 40° with a step size of 0.016°. FTIR study was performed with Perkin-Elmer spectrum one spectrometer in the range of 400−4000 cm^{-1} using KBr pellet. Field emission scanning electron microscopy (FESEM, Quanta 3D) imaging was used to examine the morphology of the synthesized samples. EDX analysis was performed with Li doped Silicon X-ray detector equipped with FESEM. High-resolution micrographs were obtained with FEI Tecnai G^2 transmission electron microscope operated at 200 keV. The samples were dispersed in ethanol and drop cast over holey carbon coated copper grid (200 mesh). The samples were dried overnight in ambient atmosphere. The AFM measurements were performed in tapping mode using Park systems XE-100. For imaging, samples were placed on freshly cleaved HOPG surface by spin coating from a suspension at 2000 rpm for 20 s. Suspensions were prepared by mixing 1 mg of graphene with 10 mL of N, N-dimethyl formamide (DMF) by ultrasonication for 15 min. This suspension was diluted to a concentration of 0.02 mg/mL. Probe sonicator (Sonics, 500 W) was used for the dispersion of graphene in commercial engine oil for 60 min. Four ball tester (Magnum Engineers, Bangalore, India) was used for studying the tribological properties of graphene based engine oils. Test balls are chrome alloy steel, made from ANSI standard.

Tribological Characterization. The frictional coefficient, wear scar test, and nonseized load of the lubricating oils with additives were evaluated by a four-ball test machine (Magnum Engineers, India). The load carrying capacity was determined according to the ASTM standard (D 2783). The tester was operated with one steel ball under load rotating against three steel balls held stationary in the form of a cradle. The rotating speed is 1760 rpm. The friction and wear tests were performed with the same machine at a rotating speed of 600 rpm and under a constant load of 392 N for test duration of 60 min at a temperature of 75 °C (ASTM standard D 5183). Before operating the machine with the test balls, we cleaned the components ultrasonically with petroleum ether and rinsed with ethanol and finally dried. Three 12.7 mm diameter steel balls were clamped together and covered with the nanolubricants to be evaluated. Experimental set up of the tribotester is shown in Scheme 1 along with schematic view of four-ball assembly. Inset of optical image shows the ball cup in four ball tester.

Figure 1 shows the morphology of the graphene prepared by exfoliation of graphite oxide by focused solar radiation. High resolution FESEM image as shown in figure 1a clearly demonstrate that synthesized graphene sample was of ultrananometer dimensions and flat single flakes can be seen. Figure 1b shows TEM image of graphene which depicts the morphology of the graphene. The thickness of graphene sheets measured using HRTEM lattice imaging came out to be less than 2 nm as

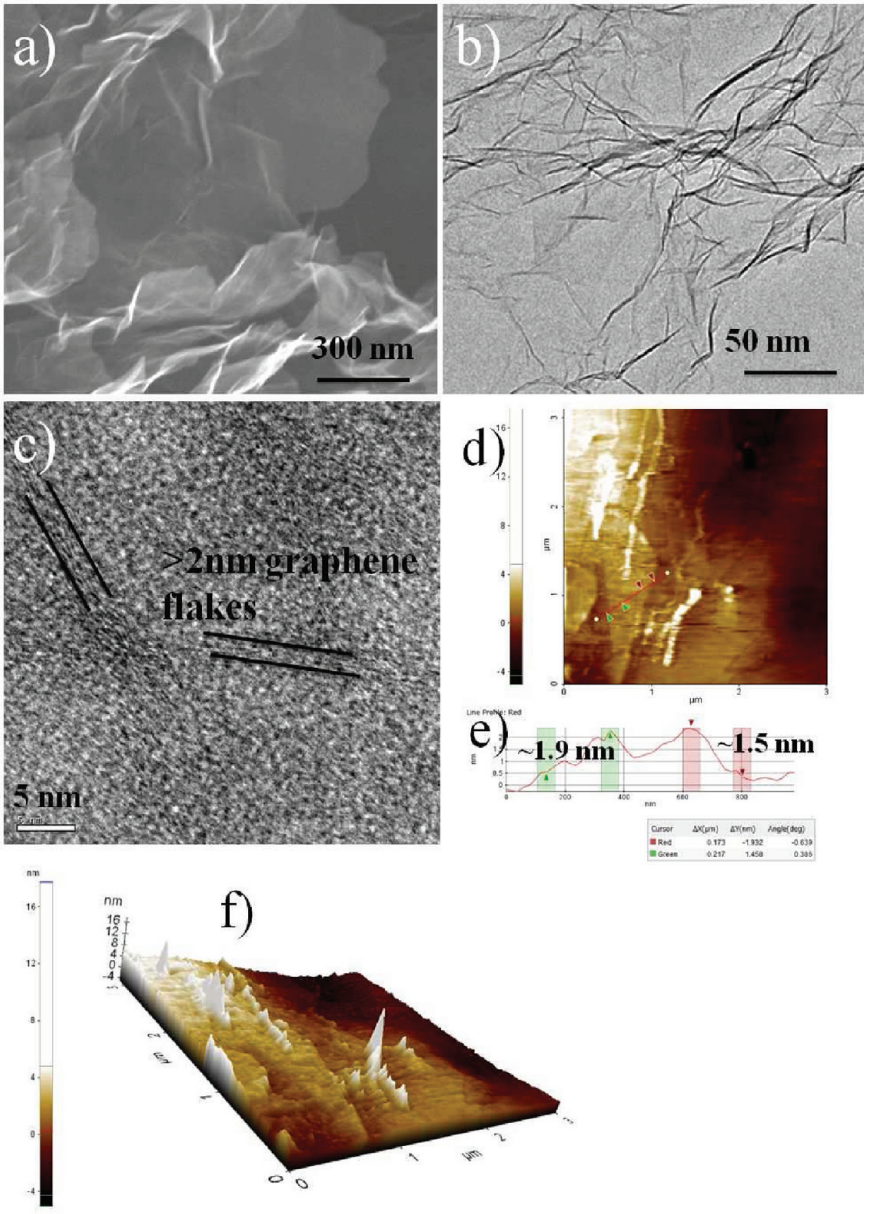

Figure 1. (a) High-resolution scanning electron micrograph of the graphene, (b) transmission electron micrograph of the graphene, (c) lattice planes of graphene, (d) atomic force microscope image of graphene in noncontact mode, (e) sectional profile of AFM image, and (f) 3D AFM image of graphene showing the islands of graphene.

shown in Figure 1c, indicating the ultrathin nature of the present solar exfoliated graphene sheets. Figure 1d−f shows the morphology and cross sectional profile, 3D view of graphene sample in noncontact mode of AFM. The average thickness of the graphene came out to be 1−2 nm[12] which is consistent with the TEM studies. The AFM 3D image shows the graphene islands at different locations.

Figure 2 shows the powder X-ray diffractograms of graphite oxide and synthesized graphene. The spectrum of GO exhibits a single peak at 10.6° for 2θ corresponding to d spacing of 8.36 Å. The increase in d-spacing value of GO can be due to the incorporation of epoxide, hydroxyl and carbonyl functional groups[32,33] between typical graphene sheets in graphite to integrate the water molecules trapped between oxygen containing functional groups in GO sheets. Because of the rapid heating of GO in the presence of focused solar radiation, the decomposition rate of the oxygen-containing groups of GO exceeds the diffusion rate of the evolved gases back to the material, thus yielding pressure that surmounts the van der Waals force holding the graphene sheets together in GO.[34] The XRD of graphene gives the complete reduction of GO, as it does not have a peak at 10.6°, yet shows a weak and broad peak C (002) around 25°. The width of the graphene peak can be due to the small size of the layers or a relatively short domain order of the stacked sheets, each of which broadens the XRD peak. Figure 2b shows the energy dispersive analysis of X-ray spectra of graphite oxide and graphene. In the case of graphite oxide, two visible peaks namely carbon and oxygen are appearing at 0.262 and 0.542 eV, respectively. On the basis of the intensity of these elements, the weight ratio of carbon and oxygen is calculated to be 70:30 and after reduction and exfoliation of graphite oxide by focused sun light, this ratio increased to ~96:4.

FTIR spectrum of graphene (Figure 3), clearly demonstrates that it does not contain any carboxyl and epoxide functional groups, which confirms its hydrophobicity. Different concentrations of graphene

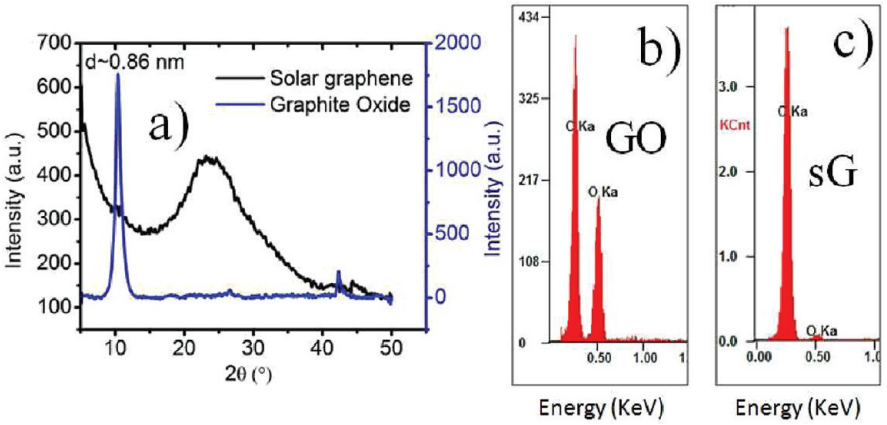

Figure 2. (a) Powder X-ray diffractograms of graphite oxide and graphene, (b, c) energy-dispersive X-ray analysis spectra of (b) graphite oxide and (c) solar graphene.

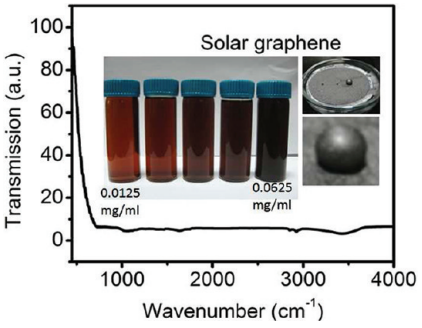

Figure 3. Fourier transform infrared spectrum of graphene; inset shows photographs of graphene-dispersed engine oil nanofluids along with water droplet on graphene film.

dispersed engine oil nanofluids are shown in the inset of figure 3 to commemorate the stability of the nanofluids. Water droplet on vacuum infiltrated graphene film was also shown, which is highly hydrophobic in nature.

The maximum, nonseized load can be defined as the load carrying capacity of the lubricant. The nonseized load for bare lubricant (base oil) is 550 N and as the concentration of graphene increases in the base oil, load carrying capacity increases initially and further decreases with increase in concentration. Much higher value in load carrying capacity of 935 N for optimal concentration of 0.025 mg/mL of solar graphene in base oil was observed. Lin et al.[29] reported with the addition of 0.075 wt % MGP to the base oil, load carrying capacity was increased from 418.5 N (for base oil) to 627.2 N (0.075 wt % MGP) and our results shows much higher performance in load carrying capacity. When the load increases, elastic deformation of the graphene takes place and it will reduce the buffering friction. And also, since thickness of graphene layers in the present case is 1−2 nm, this can form a nanobearing between moving surfaces. This may result in sliding when excess load is applied. Hence, added additive to the base oil can act as mechanical reinforcing element during friction and can therefore strengthen the load carrying capacity of the nanolubricants. When the graphene concentration is 0.025 mg/mL in base oil, the load carrying capacity is maximum. The excessive additive in base oil decreases the load carrying capacity. This can be understood as follows. When the additive is in excess, the formation of lumps in the friction interfaces will result in worse lubricating efficacy. This will further become substantial and decrease the seizing load value. Wear scar diameters

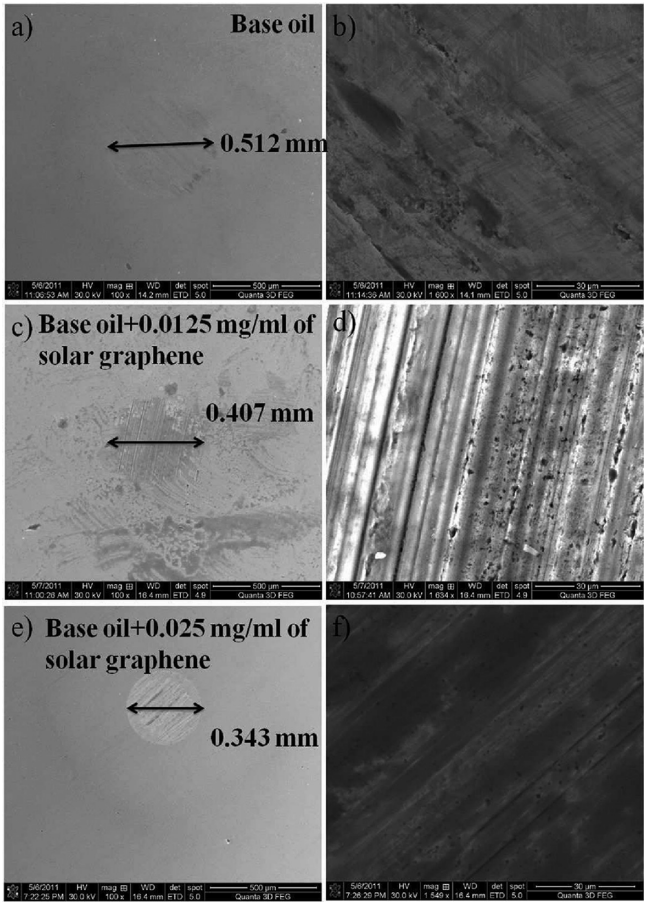

Figure 4. Wear scar diameters of stainless steel balls nano lubricated by (a) pure engine oil, (c) engine oil with 0.0125 mg/mL of solar graphene, (e) engine oil with 0.0250 mg/mL of solar graphene; (b, d, f) magnified images of a, c, and e, respectively.

of SS balls with different concentrations of graphene in base oil are shown in Figure 4. It is clear that as the graphene concentration increases in the base oil, wear scar diameter (WSD) decreases. For instance, 0.025 mg/mL concentration, WSD reduces to 0.343 mm from 0.512 mm of base oil. There is a correlation between load carrying capacity and WSD of graphene based engine oil nanofluids. Hence,

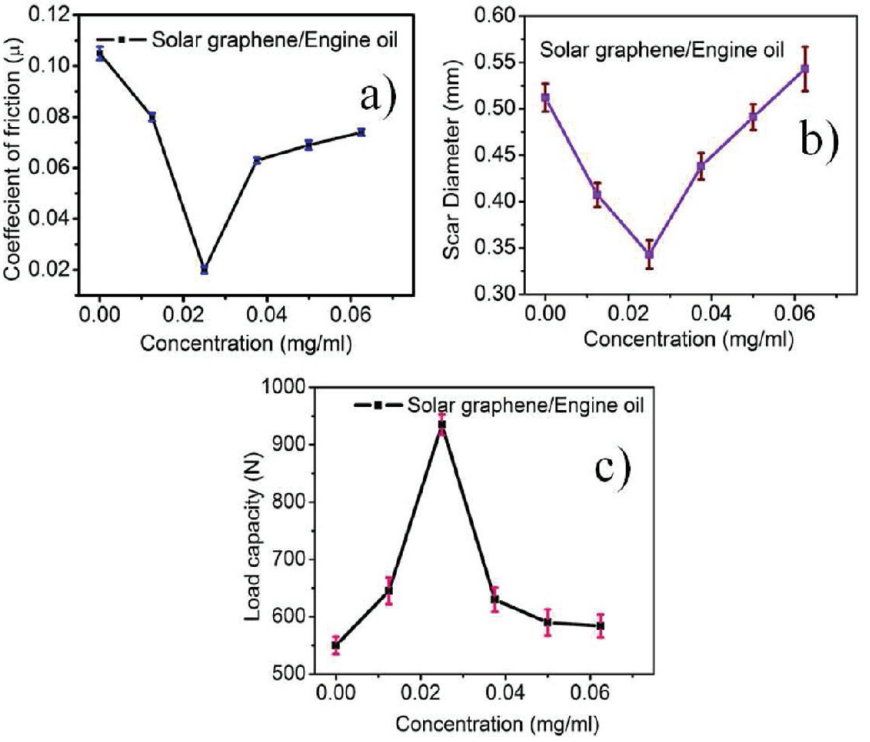

Figure 5. Tribological properties of graphene based engine oil nanofluids. (a) Coefficient of friction, (b) wear scar diameter, and (c) load capacity.

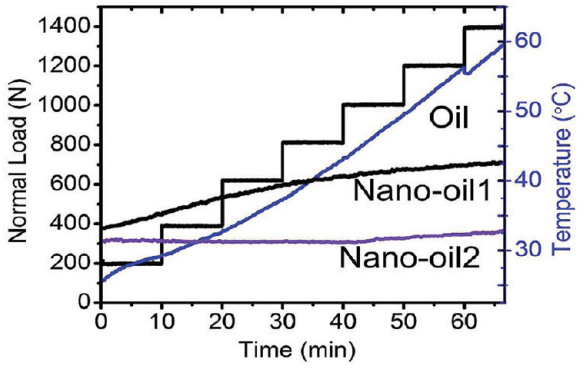

Figure 6. Comparison in surface temperature of raw oil, nano-oil 1 (0.0125 mg/mL), and nano-oil 2 (0.0250 mg/mL) as a function of normal load.

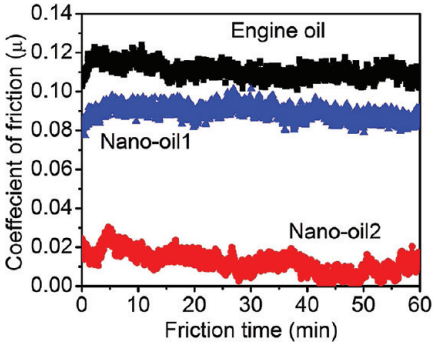

Figure 7. Coefficient of friction of graphene-based engine oil nano fluids with different concentrations of graphene (nano oil 1, 0.0125 mg/mL of graphene in engine oil; nano-oil 2, 0.025 mg/mL of graphene in engine oil).

there is an inverse relation between load carrying capacity and wear scar diameter.

Coefficient of friction (COF) for all the graphene based nanolubricants including base oil was measured using four ball tribotester and the results are displayed in Figure 5. The frictional coefficient of base oil was about 0.1. When the graphene concentration increases in the oil, initially COF decreases and reduces drastically to extremely low value at particular concentration and further it increases with increase in concentration of graphene in base oil. This enhanced decrement in frictional coefficient of graphene-oil nanolubricants can be attributed to the layered structure of graphite and due to its self-lubrication. Since, the present graphene consists of 1−2 nm layers as single flakes, it can act as nanobearing between moving parts and can reduce the friction. In the case of frictional coefficient analysis of MGP based nanolubricants, COF was decreased from 0.17 to 0.19 (base oil) to 0.12 (0.075 wt % MGP) reported by Lin et al.[29] Frictional studied reported by Pu et al.[30] are completely based on solid lubricants. Nanofriction of the lubrication films were measured using a homemade colloidal probe mounted on the same AFM in contact mode. Since, the testing method and analysis are completely different from the present study, comparable comparison between the results cannot be made. Figure 6 depicts the comparison in temperature of engine oil and graphene-oil as a function of normal load recorded during the experiment. In the case of base engine oil, the temperature increases to 60 °C at 1400 N load, but in graphene-oil 2 (0.025 mg/mL) the temperature stays around 35 °C at 1400 N load. It can be due to the polishing effect, due to which the friction coefficient decreases and hence the temperature increase is small with nano-oil. On the other hand, in the case of base engine oil, the frictional force on time was increased and hence, the temperature increases rapidly.

It is quite interesting to discuss the lubrication mechanism in graphene-based engine oil nanofluids. The above tribological experimental results suggest that both friction and wear can be dramatically improved for the optimal concentration of graphene in engine oil.[35] Solar graphene can be easily dispersed without any surfactant in the oil-based lubricants and the oil was stable for one month without much sedimentation. Even though the surface of the steel ball was looking smooth, when we observed its micrometer and nanoscale image, the surface was complicated with ridges and valleys. When these two solid surfaces were in contact, microscopically, rubbing of these ridges develops friction between the surfaces. But when we add ultrathin graphene to the base oil, it fills up the micro- and nanogaps of the rubbing surfaces so that it avoids direct contact of the two surfaces and reduces the friction and as shown in Figure 7, the frictional coefficient decreases dramatically for optimal concentration and it is constant over a period of frictional time of 60 min. A continuous lubricating film comprising of graphene was formed in the oil of rubbing surfaces. We propose that sliding is the main mechanism behind reducing friction in the case of graphene-based engine oil nanofluids. The geometry of the graphene is planar, it can easily slide between the surfaces in the oil. We could achieve best results for the optimum concentration of graphene in the base oil. Further, an increase in concentration will result in aggregation and coagulation of graphene, which will increase the wear and friction between surfaces. The noticeable decrement in wear scar diameter of steel balls can be due to the penetration of 1−2 nm graphene sheets into the contacts easily and improves the antiwear property. In the case of other carbon nanostructures like in carbon nanotubes, it is well-known that roller bearing effect is the main lubrication mechanism behind reducing friction and also there are predictions of atomistic simulations on carbon nanotubes under shear forces on tribological properties.[36−38] Analysis of the wear scar surfaces after friction confirmed that the outstanding lubrication performance of MGP could be attributed to their small size and extremely thin laminated structure, which allow the MGP to easily enter the contact area, thereby preventing the rough surfaces from coming into direct contact. During friction, the nanometer sized particles viz. carbon nanotubes and carbon nanofibers (CNFs) will first fill the microgap of the rubbing surfaces thereby forming self-assembly of lubricating thin film.[19] The phenomena of roller-bearing effect in CNTs and CNFs may improve the lubricating performance of the lubricants.

In conclusion, ultrathin graphene has been prepared by solar exfoliation technique. Different concentrations of graphene were dispersed homogeneously in base oil by probe sonication. At lesser concentrations of solar graphene, the tribological properties of graphene-engine oil nanolubricants improved enormously. For 0.025 mg/mL of graphene in engine oil, FC and WSD were reduced by 80 and 33%, respectively. This clearly demonstrates that complete reduction in frictional coefficient has been observed in the case of graphene based engine oil without modifying the surface. It was also observed that FC and WSD increases with the increase in concentration of graphene, which can be attributed to the coalesce and segregation of particles. Formation of nanobearing between the balls plays a major role in reducing the friction and wear. The excellent performance of graphene on tribological properties of these oil-based nanofluids is attributed to the ultimate mechanical strength and topological structure of graphene.

AUTHOR INFORMATION

Corresponding Author

*E-mail: ramp@iitm.ac.in. Tel: +91-44-22574862. Fax: +91-44-22570509.

ACKNOWLEDGMENT

Financial support from the Department of Science and Technology is gratefully acknowledged.

REFERENCES

(1) Novoselov, K. S.; Geim, A. K.; Morozov, S. V.; Jiang, D.; Zhang, Y.; Dubonos, S. V.; Grigorieva, I. V.; Firsov, A. A. *Science* **2004**, *306*, 666–669.
(2) Geim, A. K.; Novoselov, K. S. *Nat. Mater.* **2007**, *6*, 183–191.
(3) Lee, C.; Wei, X.; Kysar, J. W.; Hone, J. *Science* **2008**, *321*, 385–388.
(4) Eswaraiah, V.; Sankaranarayanan, V.; Ramaprabhu, S. *Macromol. Mater. Eng.* **2011**, *296*, 894–898.
(5) Eswaraiah, V.; Balasubramaniam, K.; Ramaprabhu, S. *J. Mater. Chem.* **2011**, *21*, 12626–12628.
(6) Kumar, A.; Reddy, A. L. M.; Mukherjee, A.; Dubey, M.; Zhan, X.; Singh, N.; Ci, L.; Billups, W. E.; Nagurny, J.; Mital, G.; Ajayan, P. M. *ACS Nano* **2011**, *5*, 4345–4349.
(7) Aravind, S. S. J.; Baby, T. T.; Arockiadoss, T.; Rakhi, R. B.; Ramaprabhu, S. *Thin Solid Films* **2011**, *519*, 5667–5672.
(8) Lotya, M.; King, P. J.; Khan, U.; De, S.; Coleman, J. N. *ACS Nano* **2010**, *4*, 3155–3162.
(9) Schniepp, H. C.; Li, J.-L.; McAllister, M. J.; Sai, H.; Herrera-Alonso, M.; Adamson, D. H.; Prud'homme, R. K.; Car, R.; Saville, D. A.; Aksay, I. A. *J. Phys. Chem. B* **2006**, *110*, 8535–8539.
(10) Stankovich, S.; Dikin, D. A.; Piner, R. D.; Kohlhaas, K. A.; Kleinhammes, A.; Jia, Y.; Wu, Y.; Nguyen, S. T.; Ruoff, R. S. *Carbon* **2007**, *45*, 1558–1565.
(11) Venkateswara Rao, C.; Leela Mohana Reddy, A.; Ishikawa, Y.; Ajayan, P. M. *ACS Appl. Mater. Interfaces* 2011, DOI: 10.1021/am200421h.
(12) Eswaraiah, V.; Jyothirmayee Aravind, S. S.; Ramaprabhu, S. *J. Mater. Chem.* **2011**, *21*, 6800–6803.
(13) Martin, J M, Ohmae, N *Nanolubricants*; Wiley Interscience: New York, 2008.
(14) Gao, J.; Luedtke, W. D.; Gourdon, D.; Ruths, M.; Israelachvili, J. N.; Landman, U. *J. Phys. Chem. B* **2004**, *108*, 3410–3425.
(15) Fleischauer, P. D.; Hilton, M. R. *Tribol. Int.* **1990**, *23*, 135–139.
(16) De-Xing Peng, C.-H. C.; Kang, Y.; Chang, Y.-P.; Chang, S.-Y. *Ind. Lubric. Tribol.* **2010**, *62*, 10.
(17) Chen, S.; Liu, W.; Yu, L. *Wear* **1998**, *218*, 153–158.
(18) Lu, H. F.; Fei, B.; Xin, J. H.; Wang, R. H.; Li, L.; Guan, W. C. *Carbon* **2007**, *45*, 936–942.
(19) Martorana, P.; Bayer, I. S.; Steele, A.; Loth, E. *J. Ind. Eng. Chem.* **2010**, *49*, 11363–11368.
(20) Zhang, W.; Zhou, M.; Zhu, H. W.; Tian, Y.; Wang, K. L.; Wei, J. Q.; Ji, F.; Li, X.; Li, Z.; Zhang, P.; Wu, D. H. *J. Phys. D: Appl. Phys.* **2011**, *44*, 205303.
(21) Ou, J.; Wang, J.; Liu, S.; Mu, B.; Ren, J.; Wang, H.; Yang, S. *Langmuir* **2010**, *26*, 15830–15836.
(22) Lee, C.; Li, Q.; Kalb, W.; Liu, X.-Z.; Berger, H.; Carpick, R. W.; Hone, J. *Science* **2010**, *328*, 76–80.
(23) Filleter, T.; McChesney, J. L.; Bostwick, A.; Rotenberg, E.; Emtsev, K. V.; Seyller, T.; Horn, K.; Bennewitz, R. *Phys. Rev. Lett.* **2009**, *102*, 086102.
(24) Filleter, T.; Bennewitz, R. *Phys. Rev. B* **2010**, *81*, 155412.
(25) Shen, L.; Jagota, A.; Hui, C.-Y. *Langmuir* **2009**, *25*, 2772–2780.
(26) Heim, L.-O.; Blum, J.; uuml; rgen; Preuss, M.; Butt, H.-J. *Phys. Rev. Lett.* **1999**, *83*, 3328–3331.
(27) Phil, A.; Johanna, S.; Mark, W. R. *J. Phys.: Conf. Ser.* **2007**, *61*, 51–55.
(28) Yan, X.; Perry, S. S.; Spencer, N. D.; Pasche, S.; De Paul, S. M.; Textor, M.; Lim, M. S. *Langmuir* **2003**, *20*, 423–428.
(29) Lin, J.; Wang, L.; Chen, G. *Tribol. Lett.* **2011**, *41*, 209–215.
(30) Pu, J.; Wan, S.; Zhao, W.; Mo, Y.; Zhang, X.; Wang, L.; Xue, Q. *J. Phys. Chem. C* **2011**, *115*, 13275–13284.
(31) Sun, X.; Liu, Z.; Welsher, K.; Robinson, J.; Goodwin, A.; Zaric, S.; Dai, H. *Nano Res.* **2008**, *1*, 203–212.

(32) Lerf, A.; He, H.; Forster, M.; Klinowski, J. *J. Phys. Chem. B* **1998**, *102*, 4477–4482.
(33) He, H.; Riedl, T.; Lerf, A.; Klinowski, J. *J. Phys. Chem.* **1996**, *100*, 19954–19958.
(34) Wu, Z.-S.; Ren, W.; Gao, L.; Zhao, J.; Chen, Z.; Liu, B.; Tang, D.; Yu, B.; Jiang, C.; Cheng, H.-M. *ACS Nano* **2009**, *3*, 411–417.
(35) Huang, H. D.; Tu, J. P.; Gan, L. P.; Li, C. Z. *Wear* **2006**, *26*, 140–144.
(36) Falvo, M. R.; Clary, G. J.; Taylor, R. M.; Chi, V.; Brooks, F. P.; Washburn, S.; Superfine, R. *Nature* **1997**, *389*, 582–584.
(37) Falvo, M. R.; Taylor, Ii, R. M.; Helser, A.; Chi, V.; Brooks, F. P., Jr; Washburn, S.; Superfine, R. *Nature* **1999**, *397*, 236–238.
(38) Ni, B.; Sinnott, S. B. *Surf. Sci.* **2001**, *487*, 87–96.